IR Spectroscopic and DFT Studies on the Reactions of Laser-Ablated Nb Atoms with Carbon Dioxide

Mohua Chen, Xuefeng Wang, Luning Zhang, and Qizong Qin*

Laser Chemistry Institute, Fudan University, Shanghai, 200433, China

Received: January 10, 2000; In Final Form: April 13, 2000

Reactions of laser-ablated Nb atoms with CO_2 give insertion products ONbCO and $O_2Nb(CO)_2$ and the negative species $O_2Nb(CO)_2^-$, which have been identified by matrix isolation FTIR method and DFT calculations. Two ONbCO structural products (I and II) were observed with infrared absorptions at 1902.6/960.1 and 1821.3/915.6 cm^{-1}, respectively. UV light irradiation destroyed the $O_2Nb(CO)_2^-$ anion completely, while the intensities of ONbCO(II) and O_2NbCO were enhanced markedly. Sample annealing led to the obvious increase of ONbCO(II), while the ONbCO(I) can further combine with CO_2 to form $O_2Nb(CO)_2$.

1. Introduction

As a naturally abundant carbon source in the atmosphere, carbon dioxide has received extensive consideration for its possible application to synthesizing useful organic compounds,[1−3] but due to its inherent thermodynamic stability, effective ways should be explored to activate and convert carbon dioxide into useful organic compounds. In recent decades, metal catalytic activation of carbon dioxide has been receiving increased attention.[2−4] Both the theoretical and experimental studies have been carried out to investigate the interactions between CO_2 and transition metals. [5−14] Mascetti and co-workers investigated the reactions of thermally evaporated first transition metals with pure CO_2 molecules, using matrix isolation FTIR spectroscopy.[5,6] They first observed the insertion of transition metals (M = Ti, V, and Cr) into CO_2 to form the OMCO molecules, which can be fixed by another CO_2 molecule to form (O)M(CO)(CO_2), while late transition metal atoms (M = Fe, Co, Ni, and Cu) only formed one-to-one M(CO_2) complexes. In CO_2/Ar matrixes, the reaction products mentioned above could still be observed except for the Ni + CO_2 system.[6] Interestingly, the addition of N_2 in the rare gas matrix can promote the CO_2 coordination with the Ni atom center.[7] Theoretical studies on the interactions of Ti + CO_2, Ni + CO_2, and Ni(N_2) + CO_2 systems also satisfactorily explained their experimental results.[7,8] With the first report of the insertion product OTiCO formed by the reaction of laser-ablated Ti and CO_2, a series of studies on the reactions of transition metals with CO_2 molecules were performed by Andrews and co-workers.[9−13] The insertion products OMCO (M = Sc−Ni, Y, Mo, and W) were observed as main products. The secondary products $O_2M(CO)_2$ also appeared in the reactions of CO_2 with Ti, V, Cr, Mn, Fe, Mo, and W atoms, showing that laser ablation is an effective method for producing reactive metal atoms for chemical reactions. More recently, the reactions of laser-ablated Ta with CO_2 have been studied in our group and a new species, $O_2Ta(CO)_2^-$ anion, was first reported along with the neutral insertion products.[14] To our knowledge, there is no report on the reaction of second-row transition metal Nb with CO_2 molecules.

In this paper, we report the reaction of laser-ablated Nb atoms with a CO_2/Ar mixture. The reaction products are trapped in an argon matrix and identified by the effects of isotopic substitution on their infrared spectra. The assignments of new ablated species are further confirmed by a comparison of the observed frequencies, relative intensities, and isotope ratios to those predicted by DFT calculations. The potential energy curves are calculated to predict the reaction channels for the formation of the ONbCO insertion product. The infrared spectroscopic character of main product ONbCO was compared with those of OVCO and OTaCO.

2. Experimental Section

The technique used for laser ablation and matrix isolation infrared spectroscopy has been described in detail previously.[15] Briefly, a niobium metal pellet (99%) was mounted on a rotating target holder. The laser beam at 532 nm was provided by the second harmonic of a Nd:YAG laser (Spectra Physics, GCR-150, 10 Hz repetition rate, 7 ns pulse duration) and focused on a rotating target through a hole in a CsI window. The laser-ablated species were co-deposited with carbon dioxide in excess argon onto the CsI window cooled to 11 K by means of a closed-cycle helium refrigerator (Air Products, 1R02W). FTIR spectra were recorded at a resolution of 0.5 cm^{-1} with a Bruker IFS 113V Fourier transform infrared spectrometer, using a DTGS detector. The fourth harmonic of a Nd:YAG laser (266 nm) was used as a photolysis source. High-purity carbon dioxide (Shanghai BOC, 99.99%) and isotopic $^{13}C^{16}O_2$ (>99%), and $^{12}C^{16}O_2$ + $^{13}C^{16}O_2$(55% + 45%), $^{12}C^{16}O_2$ + $^{12}C^{16}O^{18}O$ + $^{12}C^{18}O_2$ (^{18}O 60%) mixtures (Cambridge Isotope Laboratories) were used in different experiments.

3. Computational Details

Density functional theory calculations were performed to assign reaction products and model the reaction process. Optimized structures of the expected product molecules, their energies, frequencies, and the effects of isotopic substitution upon these frequencies were calculated using the GAUSSIAN 94 programs.[16] The B3LYP as well as BP86 functionals,[17−19] D95* basis sets for C and O atoms, and the Los Alamos ECP plus DZ basis sets (Lanl2DZ)[20] for the Nb atom were chosen.

Using the same basis sets, the potential energy curve for the Nb atom approaching CO_2 at quartet state was carried out both

* Corresponding author. E-mail:qzqin@fudan.ac.cn.

10.1021/jp000134z CCC: $19.00
Published on Web 07/11/2000

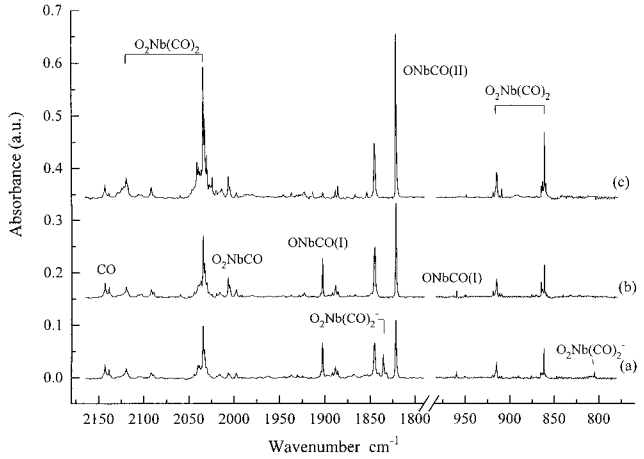

Figure 1. Infrared spectra for the matrix-isolated products from the reaction of laser- ablated Nb with 0.2% CO_2 in excess argon; (a) after 1 h of deposition at 11 K, (b) after 266 nm irradiation, (c) after annealing to 25 K.

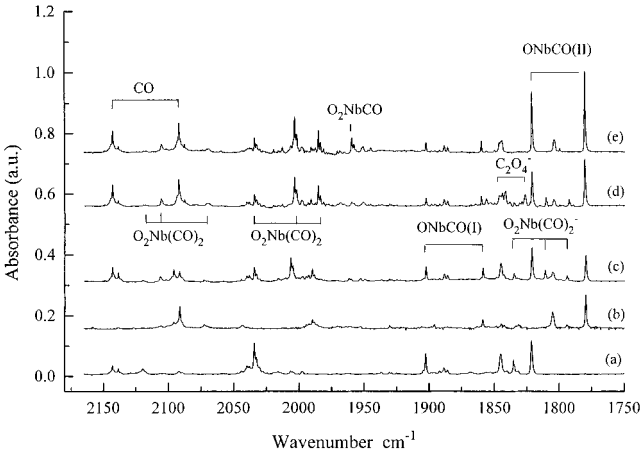

Figure 2. Infrared spectra in the 2180−1750 cm^{-1} region for the matrix-isolated products from the reaction of laser-ablated Nb with 0.2% CO_2 in argon; (a) $^{12}C^{16}O_2$, (b) $^{13}C^{16}O_2$, (c) $^{12}C^{16}O_2 + {}^{13}C^{16}O_2$, (d) $^{12}C^{16}O_2 + {}^{12}C^{16}O^{18}O + {}^{12}C^{18}O_2$, (e) 266 nm irradiation of sample (d).

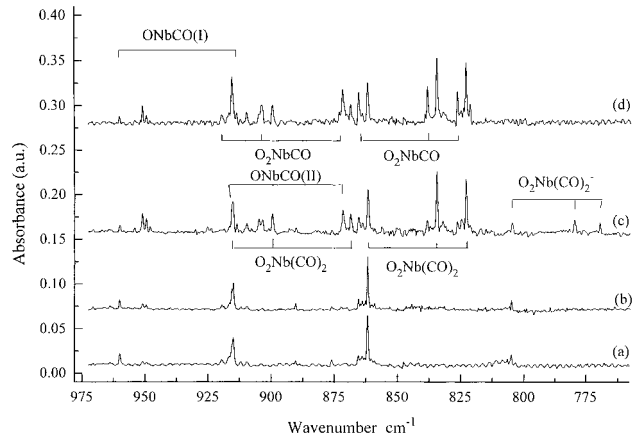

Figure 3. Infrared spectra in the 970−760 cm^{-1} region for the matrix-isolated products from the reaction of laser-ablated Nb with 0.2% CO_2 in argon; (a) $^{12}C^{16}O_2$, (b) $^{12}C^{16}O_2 + {}^{13}C^{16}O_2$, (c) $^{12}C^{16}O_2 + {}^{12}C^{16}O^{18}O + {}^{12}C^{18}O_2$, (d) 266 nm irradiation of sample (c).

by B3LYP and BP86 functionals. Though there are several different arrangements for the Nb + CO_2 reaction (the metal atom can approach the CO_2 molecule from the side-on $\eta^2_{C,O}$ direction and from the end-on η^1_C and η^1_O directions), we focus on the side-on reaction channel because it has the highest probability. The potential energy curves were calculated with respect to the reaction coordinate (R_{C-O}). The potential energy value of each point was obtained as the C−O distance was fixed and the other structure parameters were optimized.

TABLE 1: Observed Infrared Absorptions (cm^{-1}) of the Dominant Products Generated from the Reaction of Laser-Ablated Metallic Nb with a CO_2/Ar Mixture and Trapped in 11 K Ar Matrix

group	molecule	$^{12}CO_2$	$^{13}CO_2$	$^{12}CO_2/^{13}CO_2$	$C^{16}O_2/C^{16}O^{18}O/C^{18}O_2$
A	ONbCO(I)	1902.6	1858.9	1902.6, 1858.9	1902.6, 1860.4
		960.1	960.1	960.1	960.1, 913.6
B	ONbCO(II)	1821.6	1780.0	1821.6, 1780.0	1821.6, 1780.9
		915.6	915.6	915.6	915.6, 871.8
C	$O_2Nb(CO)_2$	2119.6	2072.6	2119.6, 2106.3, 2072.6	2119.6, 2106.3, 2069.4
		2034.2	1989.9	2034.2, 2006.2, 1989.9	2034.2, 2003.4, 1985.3
		2032.8	1988.2	2032.8, 2004.8, 1988.2	2032.8, 2001.9, 1983.7
		914.9	914.9	914.9	914.9, 899.7, 868.7
		861.9	861.9	861.9	861.9, 834.7, 823.1
D	$O_2Nb(CO)_2^-$	1835.3	1793.9	1835.3, 1811.3, 1793.9	1835.3, 1810.7, 1793.0
		805.1	805.1	805.1	805.1, 780.0, 769.9
E	O_2NbCO	2006.4	1961.7	2006.4, 1961.7	2006.4, 1959.7
		2004.8	1960.0	2004.8, 1960.0	2004.8, 1958.1
		919.4	919.4	919.4	919.4, 904.0, 873.2
		865.4	865.4	865.4	865.4, 838.3, 826.5
X		1845.2	1805.2	1845.2,1805.2	1845.2,1804.8

4. Results

4.1. Infrared Absorption of the Reaction Products. The FTIR spectrum of the laser-ablated Nb atoms co-deposited with 0.5 % CO_2 in 11 K argon matrix is presented in Figure 1a, and the spectra after 266 nm laser irradiation with a laser fluence of 2 mJ/cm^2 and further annealing to 25 K are shown in Figure 1b,c, respectively. The observed absorptions are listed in Table 1. In the 2180−1800 cm^{-1} region, besides the CO and $(CO)_x$ absorptions at 2138.8 and 2143.1 cm^{-1}, respectively,[10] a set of new absorptions were observed at 2119.6, 2034.2, 2032.8, 1902.6, 1845.2, 1835.3, and 1821.6 cm^{-1}. In the 1000−700 cm^{-1} region, four bands at 960.1, 915.1, 861.9, and 805.1 cm^{-1} were dominant, among which, the 915.1 cm^{-1} band can be composed of two absorptions (915.6 and 914.9 cm^{-1}), which revealed the different behavior on 266 nm irradiation and sample annealing. Irradiation (266 nm) of the deposited sample destroyed the 1835.3 and 805.1 cm^{-1} bands completely. However, the intensities of 1821.6 and 915.6 cm^{-1} bands increased markedly. In addition, three weak bands at 2006.4, 919.4, and 865.4 cm^{-1} showed about 3-fold growth. After further annealing to 25 K, the 1902.6 and 960.1 cm^{-1} bands almost vanished, while the 2119.6, 2034.2, and 1821.6 cm^{-1} as well as the 915.6, 914.9, and 861.9 cm^{-1} bands grew obviously. A two-step sample warming showed that the intensities of 1902.6 and 960.1 cm^{-1} bands increased a little at 20 K and reduced sequentially at 25 K.

Isotopic substitution experiments were done for band identification. The IR spectra were obtained using isotopic $^{13}C^{16}O_2$ and mixed $^{12}C^{16}O_2 + {}^{13}C^{16}O_2$, $^{12}C^{16}O_2 + {}^{12}C^{16}O^{18}O + {}^{12}C^{18}O_2$ samples as shown in Figures 2 and 3. The product absorptions along with their isotopic shifts are listed in Table 1. In the $^{13}CO_2$ experiment, the bands at 2034.2, 1902.6, 1845.2, 1835.3, and 1821.6 cm^{-1} shifted to 1989.9, 1858.9, 1805.2, 1793.9, and 1780.0 cm^{-1}, respectively, while no shift was observed to the

TABLE 2: Geometries (energy in kcal/mol, bond length in angstrom, angle in degree), Vibrational Frequencies (cm^{-1}), and Absorption Intensities (km mol^{-1}) of $NbCO_2$ Isomers Calculated at B3LYP Level

species	relative energy	geometry	frequencies
ONbCO(I) ($^4A''$)	0	Nb−O:1.722; Nb−C:2.144; C−O:1.163; ∠ONbC:109.6; ∠NbCO:162.7	2004.0(1558); 969.2(178); 373.3(12); 339.1(10); 299.2(0); 129.3(12)
ONbCO ($^2A'$)	+0.1	Nb−O:1.703; Nb−C:2.057; C−O: 1.168; ∠ONbC:95.5; ∠NbCO:177.9	2003.3(1175); 1013.6(149); 442.1(11); 363.3(8); 343.7(6); 159.0(8)
ONbCO(II) ($^4A''$)	+15.9	Nb−O:1.698; Nb−C:2.365; C−O:1.169; ∠ONbC:99.1; ∠NbCO:123.1	1913.3(1952); 1018.9(153); 350.3(12); 163.4(25); 104.2(3); 90.8(1)
ONb[CO] ($^2A'$)	+17.6	Nb−O:1.701; Nb−C:2.228; Nb−O:2.131; ∠ONbC:100.5; ∠ONbO:106.2	1597.1(404); 1014.8(159); 484.8(25); 395.5(11); 218.8(8); 168.7(11)
Nb[OC]O′ ($^4A'$)	+40.3	Nb−C:2.110; Nb−O:2.016; C−O′:1.194; ∠ONbC:37.8; ∠OCO′:133.0	1837.1(676); 981.4(140); 732.1(106); 430.3(0); 416.9(2); 287.2(4)
Nb[OC]O′ ($^6A'$)	+50.6	Nb−C:2.339; Nb−O:2.218; C−O′:1.194; ∠ONbC:31.6; ∠OCO′:149.1	2017.6(370); 1172.2(185); 623.1(290); 445.3(1); 330.8(5); 183.8(4)
NbOOC ($^6A'$)	+56.0	Nb−O:2.247; O−C:1.255; ∠NbOC:88.1; ∠OCO:124.6	1610.8(604); 1328.4(1); 749.1(10); 405.4(9); 346.6(59); 262.2**i**(153)
$NbCO_2$ ($^6A_1$)	+61.1	Nb−O:1.676; Nb−C:2.265; C−O:1.135; ∠ONbC:99.4; ∠NbCO:172.0	2020.6(429); 1211.1(303); 551.9(580); 504.3(2); 175.7(2); 228.1**i**(2)
$ONbCO^-$ ($^3A'$)	−30.5	Nb−O:1.748; Nb−C:2.021; C−O:1.201; ∠ONbC:106.3; ∠NbCO:167.1	1799.2(1549); 919.7(191); 462.7(8); 399.5(3); 375.0(1); 140.7(2)

TABLE 3: Geometries (energy in kcal/mol, bond length in angstrom, angle in degree), Vibrational Frequencies (cm^{-1}), and Absorption Intensities (km mol^{-1}) of $NbCO_2$ Isomers Calculated at BP86 Level

species	relative energy	geometry	frequency
ONbCO(I) ($^4A''$)	0.0	Nb−O:1.730; Nb−C:2.114; C−O:1.180; ∠ONbC:108.6; ∠NbCO:162.8	1915.6(1077); 946.8(130); 396.4(6); 343.3(5); 298.5(0); 27.5(8)
ONbCO ($^2A'$)	0.1	Nb−O:1.712; Nb−C:2.035; C−O:1.184; ∠ONbC:94.8; ∠NbCO:177.9	1918.5(824); 986.3(106); 457.9(4); 357.8(10); 341.1(9); 160.6(6)
ONbCO(II) ($^4A''$)	17.0	Nb−O:1.706; Nb−C:2.279; C−O:1.189; ∠ONbC:99.5; ∠NbCO:121.4	1811.3(1171); 995.4(114); 414.4(11); 186.9(15); 129.6(1); 98.4(1)
Nb[OC]O′ ($^6A'$)	57.4	Nb−O:2.205; Nb−C:2.314; C−O′:1.206; ∠ONbC:32.3; ∠OCO′:149.6	1963.8(297); 1129.6(138); 606.6(201); 437.1(0); 343.4(4); 186.1(3)
$ONbCO^-$ ($^3A'$)	−33.9	Nb−O:1.755; Nb−C:2.007; C−O:1.219; ∠ONbC:105.2; ∠NbCO:166.7	1725.8(1179); 900.0(144); 477.0(2); 397.4(1); 368.7(3); 141.5(1)

bands in the lower wavenumber region. In the $^{12}C^{16}O_2$ + $^{12}C^{16}O^{18}O$ + $^{12}C^{18}O_2$ experiment, all of the absorption bands exhibited isotopic shifts. It infers that all the absorptions at 2180−1750 cm^{-1} correspond to the C−O stretching modes, while those at the lower region involve only Nb and O atoms. The weak bands that appeared at 1856.7 and 1826.8 cm^{-1} in Figure 2d are due to the $C_2O_4^-$ anion.[21] Figure 2e shows that 266 nm irradiation resulted in the disappearance of $C_2O_4^-$ and two triplets at 1835.3, 1810.7, 1793.0 cm^{-1} and 805.1, 780.0, 769.9 cm^{-1}.

4.2. Calculation Results. Density functional theory calculations were employed to calculate the structures and frequencies of the possible products for confirming the experimental identification of new molecules. Five neutral $NbCO_2$ isomers were calculated, namely, ONbCO, ONb[η^2-CO], Nb[η^2-OC]O, Nb[η^1-CO_2], and Nb[η^2-OO]C. The geometries, relative energies, vibrational frequencies, and intensities calculated at B3LYP and BP86 levels are listed in Tables 2 and 3, respectively. Among these isomers, the inserted ONbCO species are more stable than any of the others. Both the doublet and quartet ONbCO have very close energy and CO stretching fundamental, so it is difficult to determine which one is the ground state. The optimization of quartet state ONb[η^2-CO] yielded a species quite different from a side-bonded structure, but close to an end-bonded structure, which is labeled as ONbCO(II) to distinguish it from the inserted ONbCO at the quartet state labeled as ONbCO(I) in the following text. The ONbCO(II) is 15.9 kcal/mol higher than the ONbCO(I) and has C−O and Nb−O stretching vibrations at 1913.3/1018.9 cm^{-1} (B3LYP) and 1811.3/995.4 cm^{-1} (BP86). The ground-state Nb[η^2-OC]O is also stable with a relative lower C−O vibration at 1837.1 cm^{-1} (B3LYP), but 40 kcal/mol higher than the ONbCO(I). Both the Nb[OO]C and $NbCO_2$ have even higher energies and one imaginary vibration for each, showing that they are not at the minimum of the potential energy surface. The ground-state $ONbCO^-$ ($^3A'$) anion was also calculated, with the CO and NbO stretching at 1799.2/919.7 cm^{-1} (B3LYP).

The theoretical predicted structures and fundamental frequencies of $O_2Nb(CO)_2$, $O_2Nb(CO)_2^-$, and O_2NbCO are listed in Table 4, and were calculated at doublet, singlet, and doublet state with C_{2v} symmetry, respectively.

Two smooth potential energy curves were obtained for the Nb + CO_2 system calculated by B3LYP and BP86 methods as shown in Figure 4. In each case, the potential energy curve reduces smoothly along with the lengthening of the C−O bond and reaches a minimum at about 1.35 Å. The optimized structure at this minimum corresponds to the side-on Nb[OC]O complex. A reaction barrier with a height of 3 kcal/mol (BP86) to 5 kcal/mol (B3LYP) exists with the R(C−O) at 1.75 Å on the potential energy curve. However, further lengthening of the C−O distance will reach an even lower minimum at 3.10 Å or so, corresponding to the equilibrium structure of ONbCO (I).

5. Discussion

5.1. Product Assignments. On the basis of the behavior upon 266 nm laser irradiation and sample annealing, the major absorption bands can be classified into five groups; these are labeled A−E in Figure 1. By making a comparison of the observed and calculated frequencies as well as the isotopic ratios listed in Table 5, the following reaction products will be identified.

ONbCO(I). Group A has two absorptions at 1902.6 and 960.1 cm^{-1}. In the $^{13}CO_2$ experiment, the upper band shifted to 1858.9 cm^{-1}, and the $^{12}C/^{13}C$ isotopic ratio 1.02351 is slightly higher than that of diatomic CO (1.02257), indicating that this is a

TABLE 4: Calculated Geometries (energy in hartree, bond length in angstrom, angle in degree),[a] Vibrational Frequencies (cm^{-1}), and Absorption Intensities (km mol^{-1}) of $O_2Nb(CO)_2^-$, $O_2Nb(CO)_2^-$, and O_2NbCO

			frequency (cm^{-1})	
molecule	total energy	geometry	B3LYP	BP86
$O_2Nb(CO)_2$ ($^2A'$)	−433.5635	C−O:1.147	2163.3(300); 2077.7(1927)	2064.6(243); 1993.4(1490)
		Nb−C:2.259	957.2(75); 912.3(214)	919.8(43); 879.5(160)
		Nb−O: 1.752	373.8(5); 330.0(4)	374.5(2); 347.3(10)
		∠OCNb:174.7	321.8(22); 307.7(4)	330.1(5); 301.2(3)
		∠CNbC:101.3	303.2(4); 295.7(5)	295.7(0); 288.2(1)
		∠ONbC:110.4	260.8(3); 98.9(0)	259.4(3);96.5(0)
		∠ONbO:127.1	94.2(22); 76.4(5); 51.5(0)	94.3(20); 72.7(4); 50.0(0)
$O_2Nb(CO)_2^-$ ($^1A'$)	−433.6601	C−O:1.172	2022.0(459); 1929.1(1914)	1931.2(400); 1855.2(1476)
		C−Nb:2.148	887.0(83); 851.1(294)	852.2(50); 821.6(231)
		Nb−O:1.797	516.8(6); 403.9(8)	505.6(4); 413.5(2)
		∠OCNb:176.0	401.4(5); 381.0(3)	401.7(5); 369.6(1)
		∠CNbC:92.1	352.6(0); 352.4(8)	345.6(7); 343.0(0)
		∠ONbC:109.6	234.1(7); 125.8(12)	266.9(6); 122.8(11)
		∠ONbO:136.5	118.8(0); 94.3(3); 66.0(0)	115.5(0); 90.8(2); 63.1(0)
O_2NbCO ($^2A'$)	−318.2278	C−O:1.153	2074.1(1444)	1989.0(1044)
		C−Nb:2.201	968.2(73); 915.0(230)	936.1(42); 888.8(175)
		Nb−O:1.747	362.9(7); 324.3(2)	378.9(2); 326.7(1)
		∠OCNb:167.8	310.8(2); 279.8(6)	305.0(1); 279.0(4)
		∠CNbO:103.4	112.1(25); 101.0(1)	118.8(21); 103.0(0)
		∠ONbO:115.4		

[a] Calculated at the B3LYP level.

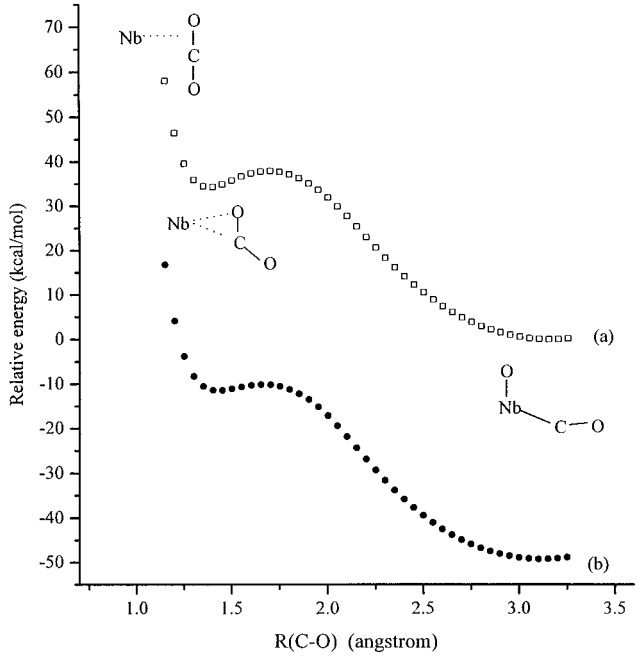

Figure 4. The calculated potential energy curves for the Nb + CO_2 reaction. All parameters are optimized with the *R*(C−O) fixed. (a) B3LYP method, (b) BP86 method.

terminal C−O stretching vibration. Experiments with $^{12}CO_2$ + $^{13}CO_2$ and $C^{16}O_2 + C^{16}O^{18}O + C^{18}O_2$ mixtures revealed isotopic doublets with similar band shape and intensity, confirming that only one CO group is involved in this mode. The 960.1 cm^{-1} band showed no shift to 13-C substitution, but the $C^{16}O_2$ + $C^{16}O^{18}O + C^{18}O_2$ experiment gave a 1:1 doublet (960.1, 913.6 cm^{-1}). The $^{16}O/^{18}O$ isotopic ratio (1.05024) is close to that of free NbO (1.0510),[22] indicating that it is a terminal Nb−O stretching vibration. So these two bands could be assigned to C−O and Nb−O vibrations of the inserted ONbCO molecule. Our DFT calculations on the $NbCO_2$ isomers showed that the most stable ONbCO(I) structure has the ν_{CO} and ν_{NbO} at 2004.0/969.2 cm^{-1} (B3LYP) and 1915.6/946.8 cm^{-1}(BP86), respectively. These frequencies, as well as the $^{12}C/^{13}C$ and $^{16}O/^{18}O$ isotopic ratios reproduce the experimental data of group A very well, which further confirms that group A is an inserted ONbCO product.

ONbCO(II). Two absorptions of group B were observed at 1821.6 and 915.6 cm^{-1}, and both of them were lower than the corresponding absorptions of group A. Their intensities increased obviously after 266 nm irradiation and sample annealing. In the $^{13}CO_2$ experiment, the 1821.6 cm^{-1} band shifted to 1780.0 cm^{-1} and exhibited 1:1 doublet structures in $^{12}CO_2$ + $^{13}CO_2$ and $C^{16}O_2 + C^{16}O^{18}O + C^{18}O_2$ experiments. The isotopic ratios of this band (1.02346 for $^{12}C/^{13}C$, 1.02280 for $^{16}O/^{18}O$) are very close to the corresponding values of the CO stretching of ONbCO(I). The 915.6 cm^{-1} band showed no shift to 13-C substitution, but a doublet (915.6, 871.8 cm^{-1}) was observed in the $C^{16}O_2 + C^{16}O^{18}O + C^{18}O_2$ experiment with the $^{16}O/^{18}O$ ratio of (1.05024), indicating that this is a Nb−O stretching mode. So there is one C−O and one Nb−O unit involved in group B, just like the ONbCO(I) mentioned above. As shown in Table 2, except ONbCO(I), the ONbCO(II) structure is more energetically favorable than other isomers. Its calculated CO stretching fundamental (1903.3 cm^{-1} for B3LYP, 1811.3 cm^{-1} for BP86) is very close to the observed 1821.6 cm^{-1} of group B. However, the calculated Nb−O stretching is higher than the experimental data. We now tentatively assign group B to the ONbCO(II) structure.

$O_2Nb(CO)_2$. Four bands of group C at 2119.6, 2034.2, 914.9, and 861.9 cm^{-1} increased apparently at the same rate on sample annealing. The upper two bands shifted to 2072.6 and 1989.9 cm^{-1} in the $^{13}CO_2$ experiment and produced triplet isotopic structures with a 1:2:1 ratio in the $^{12}CO_2$ + $^{13}CO_2$ and $C^{16}O_2$ + $C^{16}O^{18}O + C^{18}O_2$ experiments. The two lower bands showed no 13-C shift, but the $C^{16}O_2 + C^{16}O^{18}O + C^{18}O_2$ experiment gave 1:2:1 triplets to both of them, indicating the presence of two equivalent CO groups and two equivalent O atoms combined with one Nb atom. The shapes of triplet structures of two Nb−O stretchings are similar to those of the NbO_2 molecule.[22] The $^{16}O/^{18}O$ ratios of the upper 914.9 cm^{-1} (1.05318) and the lower 861.9 cm^{-1} (1.04714) absorptions are close to those of symmetric and antisymmetric vibrations of NbO_2 (1.0525 for 933.5 cm^{-1} and 1.0484 for 875.9 cm^{-1}). In view of these facts, the four bands are suitable for assignment

TABLE 5: Comparison of the Observed and Calculated Vibrational Frequencies(cm^{-1}) and Isotopic Ratios for the Observed Laser-Ablation Products

			calcd		$^{12}C/^{13}C$		$^{16}O/^{18}O$	
molecule	mode	obsd	B3LYP	BP86	obsd	calcd	obsd	calcd
ONbCO(I)	ν_{C-O}	1902.6	2004.0	1915.6	1.02351	1.02344	1.02268	1.02375
	ν_{Nb-O}	960.1	969.2	946.8	1.00000	1.00090	1.05090	1.05105
ONbCO(II)	ν_{C-O}	1821.6	1913.3	1811.3	1.02337	1.02264	1.02285	1.02495
	ν_{Nb-O}	915.6	1018.9	995.4	1.00000	1.00000	1.05024	1.05123
$O_2Nb(CO)_2$	ν^s_{C-O}	2119.6	2163.6	2064.6	1.02268	1.02370	1.02426	1.02419
	ν^{as}_{C-O}	2034.2	2077.7	1993.4	1.02226	1.02284	1.02463	1.02481
	ν^s_{Nb-O}	914.9	957.2	919.8	1.00000	1.00000	1.05318	1.05279
	ν^{as}_{Nb-O}	861.9	912.3	879.5	1.00000	1.00000	1.04714	1.04634
$O_2Nb(CO)_2^-$	ν^s_{C-O}	no[a]	2022.0	1931.2	1.02308	1.02386	1.02359	1.02312
	ν^{as}_{C-O}	1835.3	1929.1	1855.2		1.02333		1.02389
	ν^s_{Nb-O}	no[a]	887.0	852.2	1.00000	1.00001	1.04572	1.05462
	ν^{as}_{Nb-O}	805.1	851.1	821.6		1.00002		1.04648
O_2NbCO	ν_{C-O}	2006.4	2074.1	1989.0	1.02279	1.02314	1.02383	1.02420
	ν^s_{Nb-O}	919.4	968.2	936.1	1.00000	1.00000	1.05291	1.05327
	ν^{as}_{Nb-O}	865.4	915.0	888.8	1.00000	1.00000	1.04707	1.04829

[a] no = not observed in this work.

to the $O_2Nb(CO)_2$ molecule. This assignment is confirmed by the DFT calculations, which showed that $O_2Nb(CO)_2$ with C_{2v} symmetry has symmetric and antisymmetric C−O vibrations at 2163.6 and 2077.7 cm^{-1} and Nb−O vibrations at 957.2 and 912.3 cm^{-1}. For each mode, the calculated isotopic ratios match the experimental data very well.

$O_2Nb(CO)_2^-$. Group D involves a medium band at 1835.3 cm^{-1} and a very weak band at 805.1 cm^{-1}. Both bands were photosensitive to the 266 nm light irradiation. In the $^{13}CO_2$ experiment, only the 1835.3 cm^{-1} absorption shifted to 1793.9 cm^{-1}, while there were no changes for the 805.1 cm^{-1} band. In the $^{12}CO_2 + {}^{13}CO_2$ experiment, the 1835.3 cm^{-1} absorption showed triplet structure with bands at 1835.3, 1811.3, 1793.9 cm^{-1}. In the $^{12}C^{16}O_2 + {}^{12}C^{16}O^{18}O + {}^{12}C^{18}O_2$ experiment, both bands exhibited triplet structures at 1835.3, 1810.7, 1793.0 cm^{-1} and 805.1, 780.0, 769.9 cm^{-1}, respectively, characterizing that these two vibrations involve two equivalent CO groups and two equivalent O atoms, respectively. The photosensitive evidence implies that it may be due to a Nb-containing anion. The $O_2Nb(CO)_2^-$ anion is predicted by B3LYP and BP86 calculations at C_{2v} symmetry, which has two C−O and two Nb−O stretching vibrations at 2022.0, 1929.1, 887.0 851.1 cm^{-1} (B3LYP) and 1931.2, 1855.2, 852.2, 821.6 cm^{-1} (BP86). The 18-O shifts (24.6 and 42.3 cm^{-1}) for the observed 1835.3 cm^{-1} band are close to the calculated 27.7 and 45.0 cm^{-1} for 1929.1 cm^{-1} (ν^{as}_{CO}) of $O_2Nb(CO)_2^-$, while the 18-O shifts (25.1, 35.2 cm^{-1}) for the lower 805.1 cm^{-1} band are in good agreement with the calculated 28.2 and 36.8 cm^{-1} for the 851.1 cm^{-1} band (ν^{as}_{NbO}) of $O_2Nb(CO)_2^-$. The isotopic ratios of the observed upper band (1.02308 for $^{12}C/^{13}C$, 102359 for $^{16}O/^{18}O$) are very close to the calculated 1.02334 and 1.02389 for ν^{as}_{CO} of $O_2Nb(CO)_2^-$, and 1.04572 ($^{16}O/^{18}O$) for the lower band is also close to the calculated 1.04648 for ν^{as}_{NbO} of $O_2Nb(CO)_2^-$, further confirming that the two observed bands are due to the antisymmetric C−O and Nb−O stretchings of $O_2Nb(CO)_2^-$. The intensities of symmetric C−O and Nb−O stretchings are calculated to be much weaker than antisymmetric C−O and Nb−O stretchings, respectively, which could not be observed in the infrared spectra.

O_2NbCO. Three bands of group E at 2006.4, 919.4, and 865.4 cm^{-1} were very weak after deposition, but increased 3-fold after 266 nm irradiation. The $^{12}CO_2 + {}^{13}CO_2$ and $C^{16}O_2 + C^{16}O^{18}O + C^{18}O_2$ experiments gave doublet bands with a 1:1 ratio for 2006.4 cm^{-1}, indicating that only one C−O stretching is involved in this vibration. Another two bands showed no shift in the $^{13}CO_2$ experiment. However, two triplet structures with 1:2:1 ratios were observed in the $C^{16}O_2 + C^{16}O^{18}O + C^{18}O_2$ experiment with $^{16}O/^{18}O$ isotope ratios of 1.05291 for 919.4 cm^{-1} and 1.04707 for 865.4 cm^{-1}, which are in good agreement with the symmetric and antisymmetric vibrations of NbO_2. These three bands could be assigned to the O_2NbCO molecule, which is confirmed by the calculated fundamentals and corresponding isotopic ratios of O_2NbCO.

Other Products. A band with medium intensity was observed at 1845.2 cm^{-1}. Its $^{12}C/^{13}C$ (1.02216) and $^{16}O/^{18}O$ (1.02238) ratios also indicated that it is a CO stretching vibration. No other absorption was observed having the same changing rate as the 1845.2 cm^{-1} band, on annealing or laser irradiation. This band was not always observed during 11 K deposition. In the complementary experiment of Nb + CO, no absorption at 1845.2 cm^{-1} was observed. A further investigation should be performed to assign this band.

5.2. Comparison of the Nb, Ta, and V + CO_2 Systems. It is interesting to note that except for the absorptions of ONbCO-(II), the infrared spectra of the Nb + CO_2 system are very similar to those of the Ta + CO_2 system. This evidence suggests that there are similarities between these two atoms, just as between the Zr and Hf atoms, which are named the chemical "twins" of the periodic table.[23,24] Among the CO and MO (M = V, Nb, and Ta) stretching vibrations of OVCO (1881.1/974.8 cm^{-1}), ONbCO (1902.6/960.1 cm^{-1}), and OTaCO (1887.3/967.3 cm^{-1}), the CO stretching vibration has an increase trend in the order of V < Ta < Nb, while the MO stretching vibration has a reduced trend in the same order. The order reversion for Nb and Ta also exists in the vibration frequencies of other products, which results from the lanthanide contraction and relativistic effect for Ta atom.[22] The red shift of CO vibration in OMCO compared to free CO molecule is determined by the interaction of the CO unit with the Nb or Ta atom. For the atoms with the same electronic configuration, the interaction between metal atom and CO group is mainly determined by the size of the metal atom. Due to the lanthanide contraction, the bond distances of Ta−O and Ta−CO in OTaCO are even shorter than the corresponding ones in ONbCO, which lead to the relative strong interactions of Ta−CO and Ta−O bonds with respect to those of Nb−CO and Nb−O bonds.

5.3. Reaction Channels. Different from the thermal evaporation process, the interaction of high-power pulsed laser beam with a metal target produces a plasma plume containing energetic electrons, neutral atoms, and ions in both ground and

excited states,[25] so that the reactions occurring in the laser ablation process are more complicated than in the thermal evaporation process. Moreover, the reactant CO_2 gas can capture the ablated electrons to form CO_2^- or $C_2O_4^-$ anions.

$$CO_2 + e \rightarrow CO_2^- \quad (1)$$

$$2CO_2 + e \rightarrow C_2O_4^- \quad (2)$$

Previous studies on the reactions of laser-ablated metal atoms with CO_2 molecules proposed that the OMCO products could be formed from the insertion of neutral metal atoms into CO_2 molecules.[10−14] Similarly, the energetic Nb atoms can react directly with CO_2 to form ONbCO product. According to the potential energy curves shown in Figure 4, when the Nb atom approaches the CO_2 molecule, a side-on coordinated Nb[OC]O complex is possible to be formed. This complex is stable on the potential energy curve, and its further conversion to inserted ONbCO should overcome a reaction barrier with a height of 3−5 kcal/mol. It is well-known that the laser-ablated Nb atoms possess high translational energy; the reaction of Nb + CO_2 can easily overcome the energy barrier to form ONbCO(I) product. This may be the reason no Nb[OC]O complex was observed in our infrared spectra. So the major reaction channel for the formation of ONbCO(I) can be expressed by

$$Nb + CO_2 \rightarrow Nb[OC]O \rightarrow ONbCO(I) \qquad \Delta E = -57.7 \text{ kcal/mol} \quad (3)$$

When the deposited sample was annealing to 25 K, the ONbCO-(I) product disappeared completely, while the $O_2Nb(CO)_2$ increased markedly. It is reasonable to consider that this ONbCO(I) can further insert a CO_2 molecule to form $O_2Nb(CO)_2$ without activation energy:

$$ONbCO + CO_2 \rightarrow O_2Nb(CO)_2 \quad \Delta E = -39.8 \text{ kcal/mol} \quad (4)$$

Besides the formation of ONbCO(I), another structural ONbCO-(II) is unexpectedly observed, with very high strong infrared intensity. The different behavior of these two species on 266 nm irradiation implies that they may come from different reaction channels. Unfortunately, without more theoretical or experimental evidence, it is difficult to suggest its formation channel.

The formation of $O_2Nb(CO)_2^-$ may result from the following channels:

$$O_2Nb(CO)_2 + e^- \rightarrow O_2Nb(CO)_2^- \quad \Delta E = -60.6 \text{ kcal/mol} \quad (5)$$

$$Nb + C_2O_4^- \rightarrow O_2Nb(CO)_2^- \quad \Delta E = -154.2 \text{ kcal/mol} \quad (6)$$

$$ONbCO + CO_2^- \rightarrow O_2Nb(CO)_2^- \qquad \Delta E = -121.0 \text{ kcal/mol} \quad (7)$$

These reactions are all exothermic. It should be noted that the intensity of the $O_2Nb(CO)_2^-$ anion only changed a little in different experiments, no matter whether the CO_2^- and $C_2O_4^-$ were formed or not, indicating that the formation of $O_2Nb(CO)_2^-$ is less dependent on the CO_2 and $C_2O_4^-$ anions. So it is reasonable to assume that reactions 6 and 7 play less importance in the formation of $O_2Nb(CO)_2^-$, and reaction 5, the electron capture of neutral $O_2Nb(CO)_2$, might be the most probable reaction channel to form $O_2Nb(CO)_2^-$.

6. Conclusion

Matrix-isolation FTIR spectroscopy and DFT calculations were used to investigate the reaction products of laser-ablated Nb atoms with CO_2 molecules, and identified the insertion products ONbCO, $O_2Nb(CO)_2$, as well as the $O_2Nb(CO)_2^-$ anion. The ONbCO is mainly formed from the reaction of Nb + CO_2 via a Nb[OC]O complex intermediate, with an activation barrier of about 3−5 kcal/mol. The ONbCO can further insert another CO_2 to form $O_2Nb(CO)_2$, while the $O_2Nb(CO)_2^-$ may be formed via the electron capture of neutral $O_2Nb(CO)_2$.

Acknowledgment. We are grateful to professor Qi-Ke Zheng and Dr. Zhou Mingfei for their helpful discussion on the results. This work is supported by the Climbing Project of China.

References and Notes

(1) Solymosi, F. *J. Mol. Catal.* **1991**, *65*, 337.
(2) Creutz, C. *Electrochemical and Electrocatalytic Reactions of Carbon Dioxide*; Sullivan, B. P., Krist, K., Guard, H. E., Eds.; Elsevier: Amsterdam, 1993.
(3) Gibson, D. H. *Chem. Rev.* **1996**, *96*, 2063.
(4) Behr, A. *Carbon Dioxide Activation by Metal Complexes*; VCH: Weinheim, Germany, 1988.
(5) Mascetti, J.; Galan, F.; Papai, I. *Coord. Chem. Rev.* **1999**, *190−192*, 557.
(6) Mascetti, J.; Tranquille, M. *J. Phys. Chem.* **1988**, *92*, 2177.
(7) Galan, F.; Fouassier, M.; Tranquille, M.; Mascetti, J.; Papai, I. *J. Phys. Chem. A* **1997**, *101*, 2626.
(8) Papai, I.; Mascetti, J.; Fournier, R. *J. Phys. Chem. A* **1997**, *101*, 4465.
(9) Chertihin, G. V.; Andrews, L. *J. Am. Chem. Soc.* **1995**, *117*, 1595.
(10) Zhou, M.; Andrews, L. *J. Am. Chem. Soc.* 1**998**, *120*, 13230.
(11) Souter, P. F.; Andrews, L. *J. Am. Chem. Soc*. **1997**, *119*, 7350.
(12) Zhou, M.; Liang, B.; Andrews, L. *J. Phys. Chem. A* **1999**, *103*, 2013.
(13) Zhou, M.; Andrews, L. *J. Phys. Chem. A* **1999**, *103*, 2066.
(14) Wang, X. F.; Chen, M. H.; Zhang, L. N.; Qin, Q. Z. *J. Phys. Chem. A* **2000**, *104*, 758.
(15) Chen, M. H.; Wang, X. F.; Zhang, L. N.; Yu, M.; Qin, Q. Z. *Chem. Phys.* **1999**, *242*, 81.
(16) Frisch, M. J.; Trucks, G. W.; Schlegel, H. B.; Gill, O. M. W.; Johnson, B. G.; Robb, M. A.; Cheeseman, J. R.; Keith, T.; Petersson, G. A.; Montgomery, J. A.; Raghavachari, K.; Al-Laham, M. A.; Zakrzewski, V. G.; Ortiz, J. V.; Foresman, J. B.; Cioslowski, J.; Stefanov, B. B.; Nanayakkara, A.; Challacombe, M.; Peng, C. Y.; Ayala, P. Y.; Chen, W.; Wong, M. W.; Andres, J. L.; Replogle, E. S.; Gomperts, R.; Martin, R. L.; Fox, D. J.; Binkley, J. S.; Defrees, D. J.; Baker, J.; Stewart, J. P.; Head-Gordon, M.; Gonzalez, C.; Pople, J. A. *Gaussian 94*, revision D.3; Gaussian, Inc.: Pittsburgh, PA, 1995.
(17) Becke, A. D. *J. Chem. Phys.* **1993**, *998*, 5648.
(18) Lee, C.; Yang, E.; Parr, R. G. *Phys. Rev. B* **1988**, *37*, 785.
(19) Perdew, J. P. *Phys. Rev. B* **1986**, *33*, 8822.
(20) Hay, P. J.; Wadt, W. R. *J. Chem. Phys.* **1985**, *82*, 270.
(21) Zhou, M.; Andrews, L. *J. Chem. Phys.* **1999**, *110*, 2414.
(22) Zhou, M.; Andrews, L. *J. Phys. Chem. A* **1998**, *102*, 8251.
(23) Kushto, G. P.; Souter, P. F.; Chertihin, G. V.; Andrews, L. *J. Chem. Phys.* **1999**, *110*, 9020.
(24) Pyykko, P. *Chem. Rev.* **1988**, *88*, 563.
(25) Lowndes, D. H.; Geohegan, D. B.; Puretzky, A. A.; Norton, D. P.; Rouleau, C. M. *Science* **1996**, *273*, 898.